

Optimization of Soil Nailing Design Considering Three Failure Modes

Hyung-Joon Seo*, In-Mo Lee**, and Seok-Won Lee***

Received November 8, 2012/Accepted April 15, 2013/Published Online January 1, 2014

Abstract

Soil nailing is a reinforcing method using the shear strength of in-situ ground and the pullout resistance of soil nailing. In the current Korean slope design standard, only the pullout failure and the shear failure are considered as the main design factors. However, in the slope of an actual construction site, multi-face excavation is executed rather than full face excavation, and face failure can therefore occur in each excavation step due to the decrease of confining pressure on the excavation face during the top-down excavation. Therefore, it is necessary to include face failure as the main design factor in the slope design. This study verifies theoretically the mechanical behavior of face failure as well as pullout failure and shear failure. The constrained conditions for each failure mode are defined, and the optimization of soil nailing design is proposed on this basis. The design variables considered for the three failure modes are the bonded length of nail, the number of nails, and the prestress. These three design variables are estimated from the optimization design procedure proposed in this study considering constrained conditions. As the optimization design procedure of soil nailing proposed in this paper considers not only the pullout and shear failures but also face failure, it could be a more satisfactory design procedure in the actual field.

Keywords: soil nailing, shear failure, pullout failure, face failure, prestress

1. Introduction

Soil nailing is a reinforcing method using the shear strength of in-situ ground and the pullout resistance of soil nailing by inserting the nail (reinforcing material) into the ground and unifying it with the ground through grouting (Xue *et al.*, 2011; Su *et al.*, 2007; Pradhan *et al.*, 2006; Yin and Su, 2006; Junaideen *et al.*, 2004). It is a passive method because it resists only when a ground displacement occurs. On the other hand, the anchor method restricts the initial ground displacement by applying the prestress in advance. In both methods, the skin friction between ground and grouting and the tensile yield load of the inserted reinforcing material are considered as the main resistances in the design. Tan and Chow (2004) classified the failure mode of ground inside the slope as pullout failure, shear failure, and face failure. Turner and Jensen (2005) then carried out field tests on the basis of these three failure modes. The Federal Highway Administration (FHWA, 1998) of USA defined the three failure modes according to failure surface as shown in Fig. 1. Pullout failure is caused by the deficiency of skin friction between ground and grouting, and shear failure is caused by the deficiency of the tensile yield load of reinforcing material.

In the current Korean slope design standard (KISTEC, 2006), only the pullout failure and the shear failure are considered as the

main design factors. However, in the slope of an actual construction site, multi-face excavation is executed rather than full face excavation, and a face failure can therefore occur in each excavation step due to the decrease of confining pressure on the excavation face during the top-down excavation. In face failure, the ground begins to fall away from the excavation face to the final total failure surface continuously as shown in Fig. 1. In this case, a method such as prestress is required to apply the confining pressure onto the excavation face. Therefore, it is necessary to include face failure as the main design factor in the slope design.

This study verifies theoretically the mechanical behavior of face failure as well as pullout failure and shear failure. The constrained conditions (stability analysis) for each failure mode are defined, and the optimization of soil nailing design is proposed on this basis. The design variables considered for the three failure modes are the bonded length of nail, the number of nails, and the prestress. These three design variables are estimated from the optimization design procedure proposed in this study considering the constrained conditions. As this study includes not only the bonded length of the nail and the number of nails but also the prestress, the face failure in each excavation step can be considered in the optimization design procedure.

*Ph.D., School of Civil, Environmental and Architectural Engineering, Korea University, Seoul 136-713, Korea (E-mail: seose2r@nate.com)

**Member, Professor, School of Civil, Environmental and Architectural Engineering, Korea University, Seoul 136-713, Korea (E-mail: inmolee@korea.ac.kr)

***Member, Professor, Dept. of Civil and Environmental System Engineering, Konkuk University, Seoul 143-701, Korea (Corresponding Author, E-mail: swlee@konkuk.ac.kr)

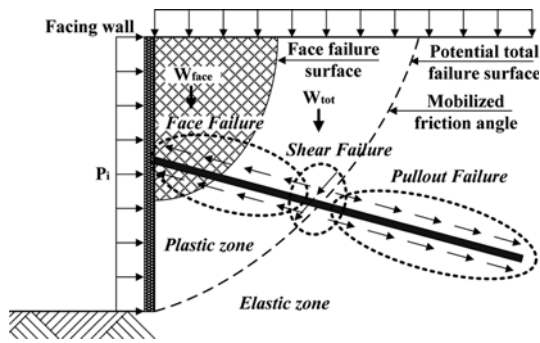


Fig. 1. Three Failure Modes

2. Constrained Conditions for Three Failure Modes

The aim of this study is to propose an optimization design procedure that considers all three failure modes in a vertical slope such as a retaining wall. To define the constrained conditions for each failure mode, a theoretical review was first conducted. For the pullout and shear failures, the resistances (skin friction and tensile strength of reinforcing material) were theoretically verified as shown in Fig. 1, to determine whether the resistances could hold the ground (soil wedge) on the potential total failure surface. In the case of face failure with multi-face excavation, as the potential failure surface can change in each excavation step, a theoretical review was carried out on the failure surface of each excavation step (rather than on the potential total failure surface) to estimate the confining pressure (such as prestress) on the excavation surface, as a design variable. Finally, by using the optimization design procedure which was induced on the basis of constrained conditions derived from each failure mode, the design variables such as bonded length of nail (X_1), number of nails (X_2), and confining pressure on excavation surface were estimated (see Fig. 2). In this study, Rankine earth pressure theory (Rankine, 1857) was used and thus the angle of failure surface (θ) in the vertical slope was

assumed as $45+\phi/2$ as shown in Fig. 7. However, this plane wedge failure mechanism can be transferred to other failure mechanisms such as log spiral mechanism. Main purpose of this paper was to suggest overall flow of optimization of soil nailing design. Therefore, plane wedge failure mechanism which is relatively simple model was used in this study. In Fig. 2, $l_1 \sim l_n$ refers to the nail length inside the failure surface; s_{min} refers to the minimum center to center distance between nails; W_{tot} is the total soil weight inside the total failure surface; L is the longitudinal length of excavated plane; H is the excavation depth; and Z is the horizontal distance from the excavation surface to total failure surface at the ground surface.

2.1 Constrained Condition for Pullout Failure

In soil nailing, the grouting is conducted after drilling the ground to resist the pullout failure through the skin friction between the ground and the grouting. The resistance to pullout failure can be divided into two elements. The first element is the resistance by shear strength (c, ϕ) of the ground itself (resistive weight by shear strength) against the total soil weight (W_{tot}) that causes the slope failure as indicated in (i) of Fig. 3. If the shear strength of ground is larger than the shear stress by soil weight, the stability is maintained and no reinforcement is needed. Otherwise, reinforcement such as soil nailing or anchor method is required. When the resistive weight by shear strength (c, ϕ) is subtracted from the total soil weight (W_{tot}), the residual soil weight ($W_{residual}$) can be obtained as in Eq. (1).

$$W_{residual} = W_{tot} \sin \theta - \frac{cL \frac{H}{\sin \theta} \tan \phi + W_{tot} \cos \theta \tan \phi}{FS_1} \quad (1)$$

Here, θ is $45+\phi/2$, ϕ is the internal friction angle, c is the cohesion, and FS_1 is the safety factor for the slope.

The second element of the resistance to pullout failure is the resistance by skin friction (T_{skin}) of soil nailing as indicated in (ii) of Fig. 3, which can be calculated with Eq. (2).

$$T_{skin} = \tau_f \frac{D\pi X_1 X_2}{FS_2} \quad (2)$$

Here, τ_f refers to the unit skin friction and FS_2 is the safety factor for pullout failure.

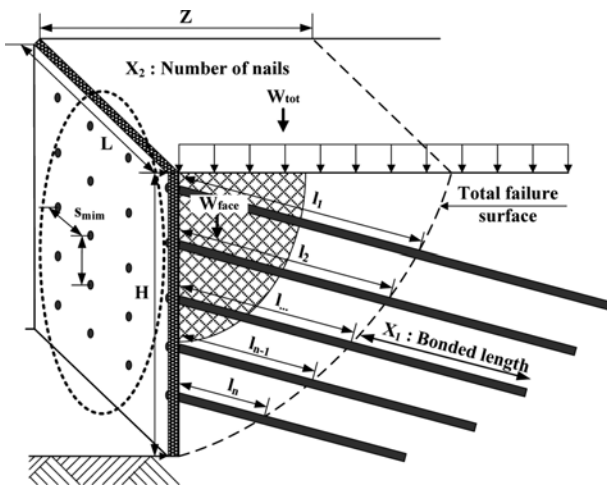


Fig. 2. Design Variables in Optimization of Soil Nailing Design

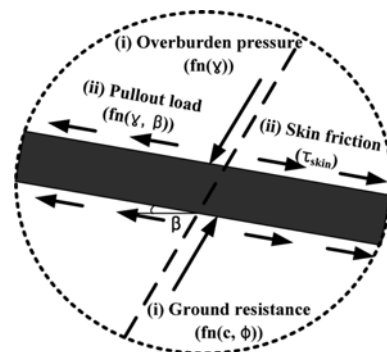


Fig. 3. Pullout Failure on Total Failure Surface

In this study, the skin friction theory proposed by Wang and Richwien (2002) is applied to obtain τ_f as in Eq. (3).

$$\tau_f = \frac{f}{1 - \left[2 \frac{(1+\nu)}{(1-2\nu)(1+2K_0)} \right] f \tan \psi} \sigma_m \quad (3)$$

Here, f is the friction angle between ground and grouting and its value is $\tan \delta$. In the case of a rough surface such as a grouting surface, δ can be regarded as ϕ (Wang and Richwien, 2002). ν is Poisson's ratio, K_0 is the coefficient of earth pressure at rest, ψ is the dilatancy angle, and σ_m is the mean normal stress onto the grouting surface.

Therefore, the constrained condition for pullout failure ($g_1(X)$) (whereby the result of subtracting the resistive weight by the skin friction of soil nailing (Eq. (2)) from the residual soil weight (Eq. (1)) should not be greater than '0') can be derived as in Eq. (4).

$$g_1(X) = \left(W_{tot} \sin \theta - \frac{cL \frac{H}{\sin \theta} \tan \phi + W_{tot} \cos \theta \tan \phi}{FS_1} \right) \times \cos \theta \times \cos \beta - \frac{f}{1 - \left[2 \frac{(1+\nu)}{(1-2\nu)(1+2K_0)} \right] f \tan \psi} \sigma_m \frac{D_p X_1 X_2}{FS_2} \leq 0 \quad (4)$$

Here, b represents the nailing angle as shown in Fig. 3.

2.2 Constrained Condition for Shear Failure

For soil nailing, various reinforcing materials with tensile strength such as steel bar, PC strands, and steel pipe are used as the nail. When a shear failure occurs on the failure surface, the reinforcing material (nail) mobilizes the tensile strength as shown in Fig. 4. That is, the earth pressure by soil weight on the nail induces the ground displacement on the failure surface. If the ground condition is as stiff as a rock showing brittle behavior, the reinforcing material may be cut by the shear stress. However, as soil nailing is generally used in the flexible ground condition showing ductile behavior, the flowing-down soil weight induces the tensile behavior of the nail by pulling down the nailed body. For this reason, in the current Korean slope design standard (KISTEC, 2006), the behavior of reinforcing material by the shear failure is not considered as a shear behavior but as a tensile behavior. Therefore, the tensile behavior theory is applied and

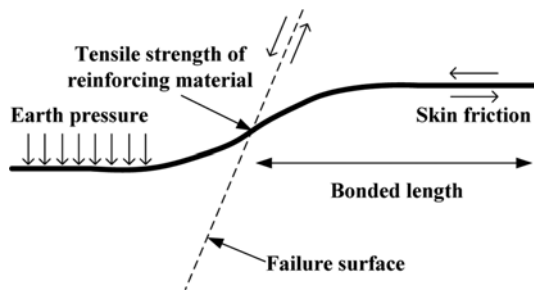


Fig. 4. Tensile Behavior of Nail due to Shear Failure

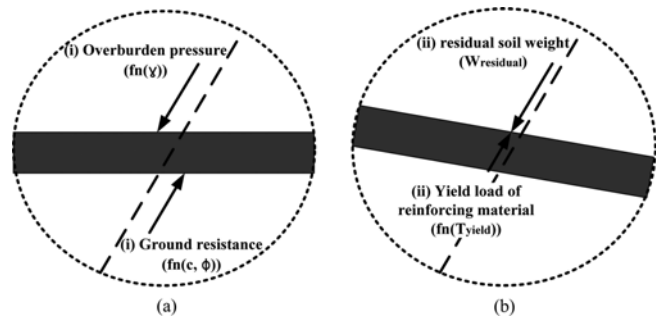


Fig. 5. Shear Failure on Total Failure Surface: (a) Resistance by Ground Itself, (b) Resistance by Reinforcing Material

developed in this study. Here, the constrained condition for shear failure can be called the constrained condition for tensile failure.

The resistance to shear failure can be divided into two elements as shown in Fig. 5. Firstly, Fig. 5(a) shows the ground itself resisting the earth pressure by soil weight. Therefore, the residual soil weight ($W_{residual}$), whereby the resistance by the shear strength of ground is subtracted from the total soil weight (W_{tot}), is the same as that in Eq. (1). Secondly, the resistance by reinforcing material against the shear failure can be represented by the yield load (tensile strength) of reinforcing material as shown in Fig. 5(b) and Eq. (5).

$$T_{tension} = \frac{T_{yield} X_2}{FS_3} \quad (5)$$

Here, $T_{tension}$ refers to the tensile strength of reinforcing material, and FS_3 is the safety factor for the shear failure.

The resistance to shear failure then resists with the tensile strength of the reinforcing material to the same extent as the residual soil weight estimated in Eq. (1), and it is presented as Eq. (6). Then, Eq. (6) becomes the constrained condition ($g_3(X)$) for the shear failure.

$$g_3(X) = \left(W_{tot} \sin \theta - \frac{cL \frac{H}{\sin \theta} \tan \phi + W_{tot} \cos \theta \tan \phi}{FS_1} \right) - \frac{T_{yield} X_2}{FS_3} \leq 0 \quad (6)$$

2.3 Constrained Condition for Face Failure

While the stability of the pullout failure and the shear failure are checked on the total failure surface after the entire excavation, the stability of the face failure is checked on every failure surface

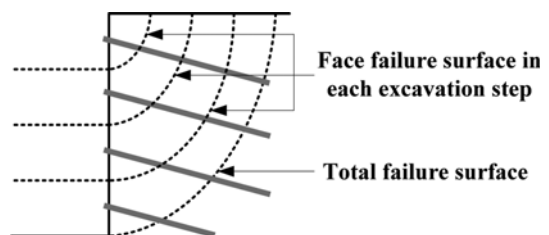


Fig. 6. Change of Failure Surface in Each Excavation Step

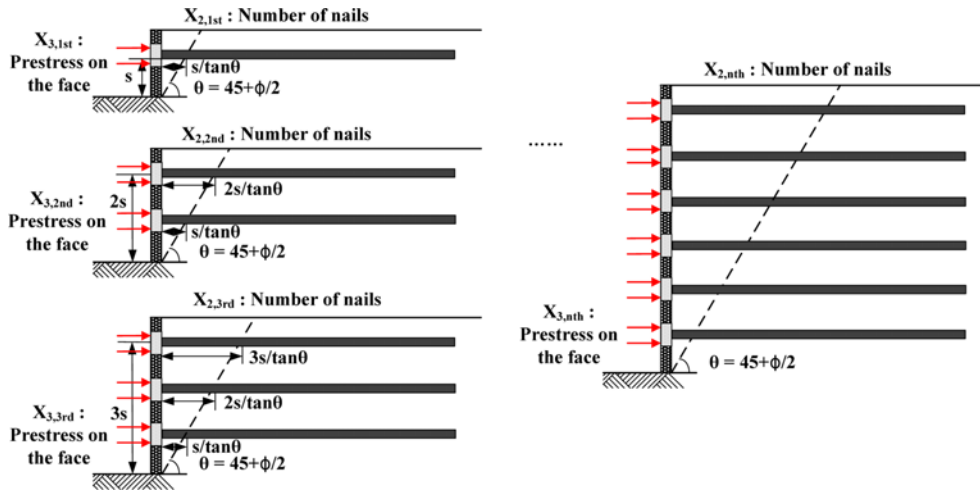


Fig. 7. Estimation of Prestress in Each Excavation Step

generated in each excavation step as shown in Fig. 6. On starting the excavation, the horizontal stress on the excavation surface becomes '0' and consequently face failure can occur. Even though reinforcing factors of inside failure which are tensile strength of reinforcement and skin friction exist, the face failure can occur by non-horizontal stress. In the end, the total failure can be induced by the expansion of the face failure. To secure the stability of the face failure, the skin friction of soil nailing (similar to Eq. (2)) should be larger than the residual soil weight (similar to Eq. (1)) induced on the face failure surface. If the skin friction is smaller than the residual soil weight, additional confining pressure such as prestress is needed. In this study, a theoretical review was carried out to estimate the required prestress in each excavation step to resist the face failure. Here, the prestress means that the reinforcing material is actively stressed in the prestressing process.

As shown in Fig. 7, face failure can occur in the 1st excavation step according to the excavation depth. As indicated in Eq. (1), face failure is first resisted by the shear strength of ground itself on the face failure surface. The skin friction of soil nailing ($T_{skin, 1st}$) mobilized outside the face failure surface in the 1st excavation step becomes Eq. (7). Here, the design variables, $X_{\square, \triangle}$ in Fig. 7 has a notation as follows: 1, 2 and 3 in \square means the bonded length of nail, the number of nails and the prestress, respectively. 1st, 2nd and nth in \triangle means the first excavation step, the second excavation step and the nth excavation step, respectively. Therefore, $X_{2, 1st}$ is the number of nails in the 1st excavation step; and s is the center to center distance between nails.

$$T_{skin, 1st} = \frac{\tau D \pi \frac{s}{\tan \theta} X_{2, 1st}}{FS_2} \quad (7)$$

If the face failure cannot be resisted by the shear strength of ground and the skin friction of soil nailing, additional confining pressure is needed as in Eq. (8). Here, $T_{prestess, 1st}$ is the total required prestress in the 1st excavation step; and $X_{3, 1st}$ is the required prestress for each nail in the 1st excavation step.

$$T_{prestess, 1st} = X_{3, 1st} \times X_{2, 1st} \quad (8)$$

Therefore, the prestress required in the 1st excavation step can be expressed as Eq. (9) by using Eqs. (1), (7), and (8).

$$h_1(X) = \left[\left(W_{tot} \sin \theta - \frac{cL \frac{H}{\sin \theta} \tan \phi + W_{tot} \cos \theta \tan \phi}{FS_1} \right) \times \cos \theta \times \cos \beta \right] - \left[\frac{\pi D \pi \frac{s}{\tan \theta} X_{2, 1st}}{FS_2} \right] - [X_{3, 1st} \times X_{2, 1st}] = 0 \quad (9)$$

In the 2nd excavation step, if there is some residual pressure even after subtracting the resistances by the ground itself, the skin frictions of soil nailing in the 1st and 2nd excavation steps, and the prestress applied in the 1st excavation step from the soil weight, the relevant pressure should be applied as the prestress on the excavation surface. When this process is repeated until the nth excavation step, the prestress required in each excavation step can be estimated as Eq. (10).

$$h_n(X) = \left(W_{tot} \sin \theta - \frac{cL \frac{H}{\sin \theta} \tan \phi + W_{tot} \cos \theta \tan \phi}{FS_1} \right) \times \cos \theta \times \cos \beta - \frac{\tau D \pi \frac{s}{\tan \theta} X_{2, 1st}}{FS_2} - \sum_{(n-1)}^1 X_{3, nth} \times X_{2, 1st} - \frac{\tau D \pi \frac{s}{\tan \theta} X_{2, nth}}{FS_2} - X_{3, nth} \times X_{2, nth} = 0 \quad (10)$$

The prestress estimated in each excavation step differs. In general, the prestress increases as it moves from the top to the bottom. Therefore, when the constructability of soil nailing is considered, it is reasonable to calculate the average prestress ($X_{3, avg}$) as in Eq. (11) and apply it uniformly in each excavation step.

$$X_{3,avg} = \frac{X_{3,1st} + X_{3,2nd} + \dots + X_{3,(n-1)th} + X_{3,nth}}{n} \quad (11)$$

The prestress must be determined as smaller than the tensile strength (yield load) of the reinforcing material (nail). Excessive prestress could be helpful in restricting the initial ground displacement; however, it reduces the tensile strength of the reinforcing material to the same extent as the applied prestress, weakening the long term slope stability. Therefore, the application of prestress obtained by using the proposed method in this study can not only prevent the face failure but also secure the long term slope stability by using the minimum tensile strength of reinforcing material.

2.4 Constrained Conditions according to Construction Conditions

Besides the constrained conditions for the pullout failure, the shear failure, and the face failure on the failure surface, additional constrained conditions can be defined according to the construction conditions. Firstly, the nails should be installed at least up to the outside of the failure surface. That is, the bonded length of nail (X_1) (see Fig. 2) should be longer than '0' as defined in Eq. (12).

$$g_2(X) = X_1 > 0 \quad (12)$$

Secondly, in the soil nailing, the reinforced boundary (nailed body) per hole differs according to the grouting method. It is

assumed that the grouting is injected into the whole borehole. When the pressurized grouting is applied, the radius of the nailed body increases and thus the distance between nails increases more than in the gravitational grouting method. Therefore, if the longitudinal length (L) and the excavation depth (H) of the excavated plane are divided by the minimum distance between nails (s_{min}), determined considering the grouting method (see Fig. 2), the constrained condition for the number of nails (X_2) can be expressed as Eq. (13).

$$g_4(X) = X_2 \leq L/s_{min} \times H/s_{min} \quad (13)$$

3. Optimization of Soil Nailing Design

In this study, the constrained conditions for the pullout failure and the shear failure on the total failure surface were defined and two additional constrained conditions were also defined according to the construction conditions. Considering these four constrained conditions on the total failure surface, the optimization design procedure for the soil nailing is derived as shown in Fig. 8. In addition, the procedure for determining the required prestress in each excavation step is proposed, considering the constrained condition for face failure as shown in Fig. 8. The design variables are the bonded length of nail (X_1), the number of nails (X_2), and prestress (X_3). The objective function can be expressed as Eq. (14).

$$f(X) = \left(\frac{l_1 + l_2 + \dots + l_{n-1} + l_n}{n} + X_1 \right) X_2 \quad (14)$$

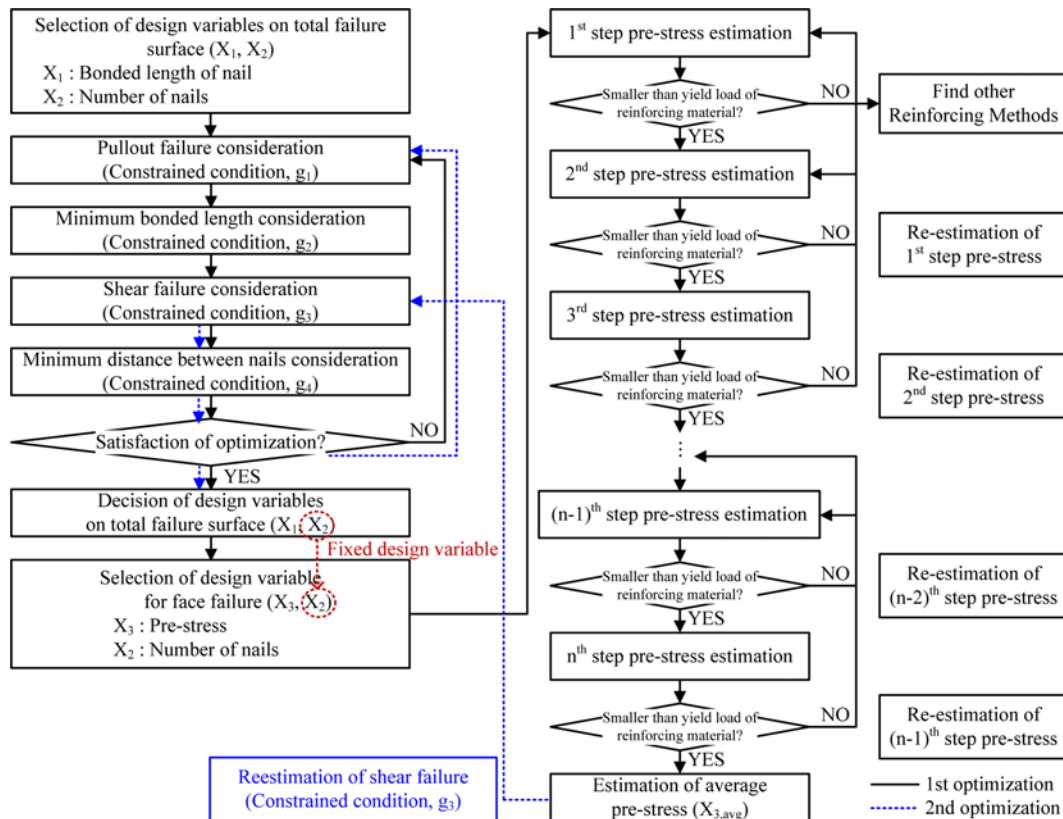


Fig. 8. Optimization Design Procedure

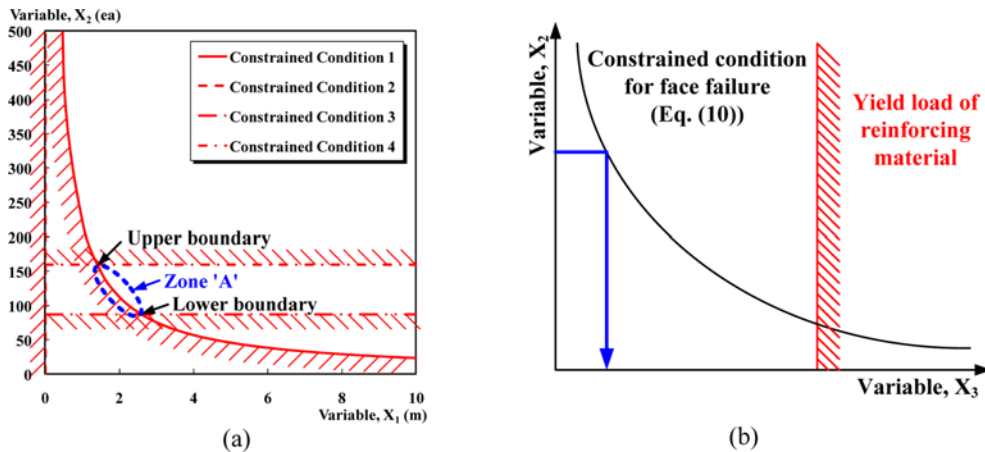


Fig. 9. Optimization of Soil Nailing Design: (a) Optimization on Total Failure Surface, (b) Estimation of Prestress

When the objective function is optimized with the four constrained conditions on the total failure surface, the upper and lower boundaries of the design variables can be determined as shown in Fig. 9(a). Consequently, the designer can choose the bonded length of nail and the number of nails on the boundary (Zone ‘A’ in Fig. 9(a)) as well as the distance between nails by arranging nails to fit the excavated plane. With the determined distance between nails and the number of nails, the number of nails to be installed in each excavation step can also be determined. If the number of nails obtained from the optimization design procedure is substituted into Eq. (10), the prestress for each excavation step can be estimated as shown in Fig. 9(b). The determined prestress in each excavation step must be smaller than the tensile strength of reinforcing material as shown in Fig. 9(b). If the estimated prestress is larger than the tensile strength, the designer should go back to the former step and increase the prestress of the former step. By repeating this process, the prestress in each excavation step can be determined. Summing up these prestresses, the average prestress is finally estimated.

Prestress is a method used to confine the ground by extending the reinforcing material. As the prestress is applied, the resistible tensile strength of the reinforcing material is decreased. Consequently, the constrained conditions for shear failure are changed and the tensile yield load of reinforcing material (T_{yield}) in Eq. (6) becomes the residual (remaining) yield load of reinforcing material ($T_{residual}$) as in Eq. (15).

$$g_3(X) = \left(W_{tot} \sin \theta - \frac{cL \frac{H}{\sin \theta} \tan \phi + W_{tot} \cos \theta \tan \phi}{FS_1} \right) - \frac{T_{residual} X_2}{FS_3} \leq 0 \quad (15)$$

Since the constrained conditions on the total failure surface are re-established in this way, the optimization design procedure should be conducted again. In other words, if the initially determined design variables (X_1, X_2) satisfy the re-established constrained conditions, the initial design variables can be determined as the final design variables. However, if the initially determined design variables do not satisfy the re-established

constrained conditions, the optimization design procedure should be repeated by changing the design variables until the estimated design variables satisfy the constrained conditions. Through this process, the design variables (the bonded length of nail (X_1), the number of nails (X_2), and the prestress (X_3)) can be determined.

4. Example of Optimization of Soil Nailing Design

The proposed optimization design procedure considering the three failure modes is applied to certain ground and construction conditions, and its procedure and results are examined to confirm the validity of the proposed optimization design procedure. The applied ground and the construction conditions are shown in Table 1 and Fig. 10. For the yield load of the nail, the properties of $\Phi 25$ mm steel bar, which has been generally used in the soil nailing, were applied. For the construction conditions, the diameter of drilling hole was assumed to be the diameter of the nailed (grouted) body and the minimum distance between nails was set as 1.5 m, which is the minimum distance between nails of general gravitational soil nailing. The safety factors were determined on the basis of those in the Korean slope design standard

Table 1. Ground and Construction Conditions

Ground Properties	Cohesion, c (kPa)	30
	Internal friction angle, ϕ ($^\circ$)	30
	Dilatancy angle, ψ ($^\circ$)	10
	Poisson's ratio, ν	0.3
	Coefficient of earth pressure at rest, K_0	0.5
	Unit weight, γ (kN/m 3)	20
Nail Properties	Yield load of steel bar (kN)	203
	Diameter of nailed body (m)	0.105
Construction Conditions	Excavation depth, H (m)	10
	Longitudinal length of excavated plane, L (m)	36
	Minimum distance between nails, s_{min} (m)	1.5
Safety Factor	Slope, FS_1	2.0
	Shear failure, FS_3	2.0
	Pullout failure, FS_2	2.0

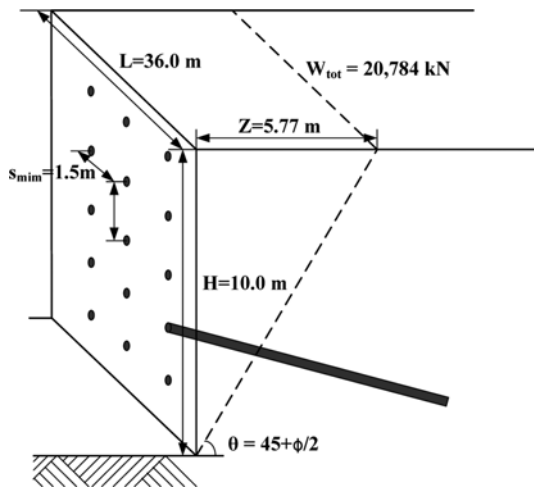


Fig. 10. Ground and Construction Conditions

(KISTEC, 2006).

When the ground and construction conditions in Table 1 are substituted into four constrained conditions of Eqs. (4), (6), (12) and (13), the upper and lower boundaries of the objective function can be obtained according to each constrained condition as shown in Fig. 11(a). The designer can select the appropriate design variables between the two boundaries on the basis of stability and economy. In this example, the 5-step excavation with 2.5 m bonded length of nail, 90 nails, and 2.0 m distance between nails was selected as shown in Fig. 11(b).

After the optimization design for the total failure surface (Fig. 11) is carried out by following the procedure as indicated in Fig. 8, the confining pressure should be estimated in each excavation step. In this example, the prestress was selected as a method of confining pressure. The prestress is estimated in each excavation step. For example, the prestress in the 1st excavation step can be

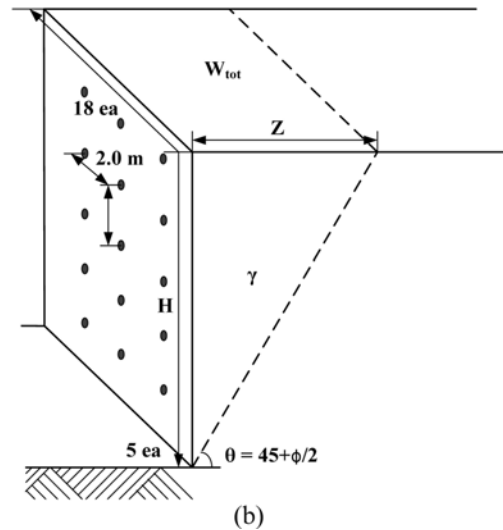
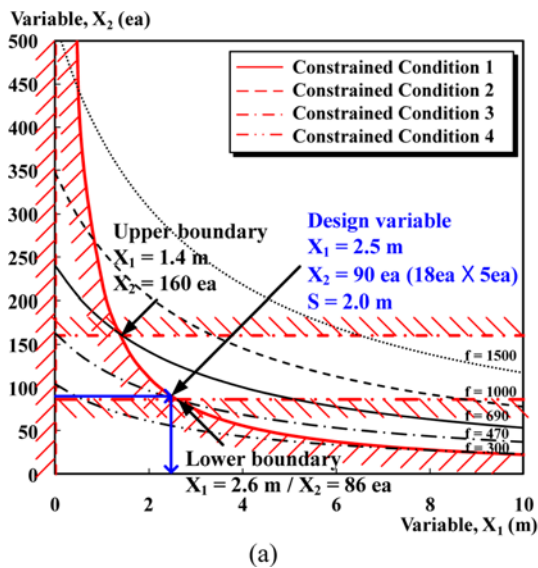


Fig. 11. Optimization Design for Total Failure Surface: (a) Application of Each Constrained Condition, (b) Selected Design Variables

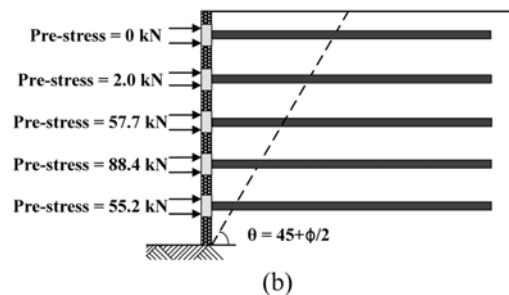
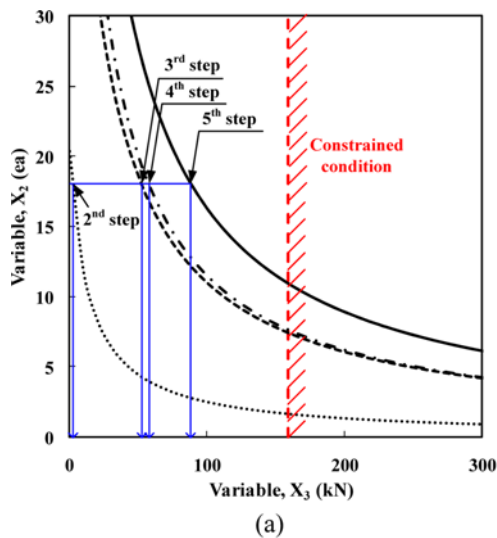


Fig. 12. Estimation of Prestress: (a) Prestress in Each Excavation Step, (b) Estimated Prestress

estimated with Eq. (10). That is, by substituting 18 as the number of nails per excavation step (which was obtained in the optimization design procedure for total failure surface as shown in Fig. 11) into Eq. (10), the prestress can be estimated. However, the estimated prestress should be smaller than the tensile strength of the reinforcing material as shown in Fig. 12.

According to Fig. 12(a), as the soil weight inducing failure is very small in the 1st excavation step, face failure does not occur even if the prestress is not applied. However, as the excavation step increases, the prestress also increases. As shown in Fig. 12(a), when the excavation step increases, the curved line obtained by Eq. (10) is shifted to the right, increasing the prestress in each excavation step. The prestress estimated in each excavation step is presented in Fig. 12(b). The average prestress estimated with Eq. (11) was about 40 kN. As shown in Fig. 8, once the prestresses are estimated, the optimization design on the total failure surface should be conducted again. This is because, as mentioned above, the application of prestress decreases the tensile strength of the reinforcing material to the same extent as the applied prestress. Therefore, the residual (remaining) tensile strength of reinforcing material becomes 163 kN, whereby the prestress was subtracted from the yield load of the reinforcing material (203 kN in Table 1).

When the constrained conditions for shear failure are re-estimated with Eq. (15), we can see in Fig. 13 that the initially estimated design variables are beyond the constrained conditions for the shear failure. That is, the reduction of tensile strength of reinforcing material by the applied prestress induces the shear failure. To satisfy the constrained conditions for the shear failure, the designer should select one of the following three methods: re-estimate the design variables from the newly-established upper and lower boundaries; increase the diameter of reinforcing material to increase the tensile strength of reinforcing material or add another reinforcing material; apply the confining pressure by using a method other than the prestress application with the

reinforcing material. By using one of these methods, the stability of soil nailing considering the three failure modes can be secured.

5. Conclusions

The aim of this study was to theoretically verify the mechanical behavior and the resistive element of face failure in soil nailing as well as other conventional design factors such as pullout failure and shear failure. With the theoretical verification of face failure, the required prestress was newly added as a design variable of soil nailing in addition to conventional variables such as the bonded length of nail and the number of nails. For the three design variables selected in this method, the optimum values were determined on the basis of constructability, stability, and economy through the optimization design procedure in consideration of the three failure modes proposed in this study. Some findings drawn from this study are as follows.

For the optimization design on the total failure surface, four constrained conditions were defined. Pullout failure occurs when the soil weight inducing failure is greater than the skin friction under the condition that the tensile strength of reinforcing material is sufficiently secured. On the other hand, shear failure occurs when the soil weight inducing failure is greater than the tensile strength of reinforcing material while the skin friction is sufficiently secured. In both failure modes, the residual soil weight after the resistance by the soil strength itself was checked to determine how much it could be resisted by the skin friction and tensile strength of the reinforcing material, and this was verified theoretically. On the total failure surface, the constrained condition for the minimum length of nail according to the construction condition and the constrained condition for number of nails according to the minimum distance between nails were also proposed.

In the slope of an actual construction site, multi-face excavation is executed via top-down excavation. Therefore, on the excavation surface, face failure can occur due to the decrease of confining pressure. To prevent this, it is necessary to apply confining pressure such as prestress on the excavation surface. In this study, a theoretical equation to obtain the reasonable confining pressure was proposed to apply the minimum necessary prestress in each excavation step.

Finally, by applying four constrained conditions and the equation for prestress estimation, the optimization design procedure of soil nailing considering three failure modes was proposed as follows. Firstly, with four constrained conditions on the total failure surface, the design variables (the bonded length of nail and the number of nails) are set as an objective function and optimized. Secondly, with the estimated number of nails, the prestress in each excavation step is estimated considering the constrained conditions for face failure. Lastly, as the applied prestress decreases the tensile strength of reinforcing material, the constrained conditions for the shear failure should be re-established and the optimization design procedure is repeated

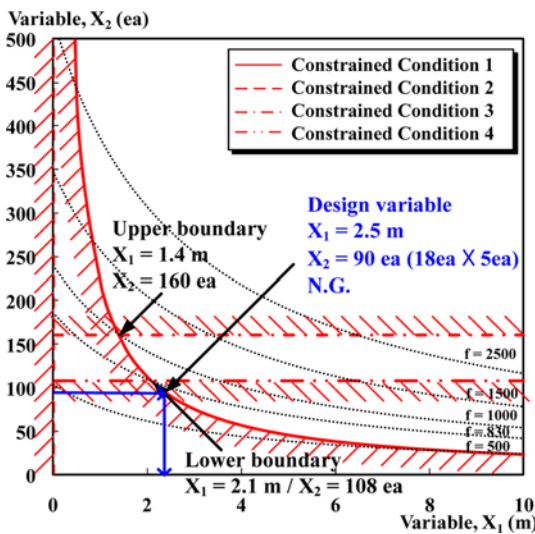


Fig. 13. Review of Initially Estimated Design Variables

until the optimum design variables are obtained. As the optimization design procedure of soil nailing proposed in this study considers not only the pullout and the shear failures but also the face failure, it could be a more satisfactory design procedure in the actual field.

Acknowledgements

This study was funded by the Korea Agency for Infrastructure Technology Advancement under the Ministry of Land, Infrastructure and Transport in Korea.

References

- FHWA (Federal Highway Administration) (1998). *Manual for design and construction monitoring of soil nail walls*, US Department of Transportation, USA.
- Junaideen, S. M., Tham, L. G., Law, K. T., Lee, C. F., and Yue, Z. Q. (2004). "Laboratory study of soil nail interaction in loose completely decomposed granite." *Canadian Geotechnical Journal*, Vol. 41, No. 2, pp. 274-286.
- KISTEC (Korea Infrastructure Safety and Technology Corporation) (2006). *Korean slope design standard*, Ministry of Land, Transport and Maritime Affairs, Korea.
- Pradhan, B., Tham, L. G., Yue, Z. Q., Junaideen, S. M., and Lee, C. F. (2006). "Soil-nail pullout interaction in loose fill materials." *International Journal of Geomechanics*, Vol. 6, Issue 4, pp. 238-247.
- Rankine, W. J. M. (1857). "On the stability of loose earth." *Philosophical Transactions of the Royal Society of London*, Vol. 147, pp. 9-27.
- Su, L. J., Chan, T. C. F., Shiu, Y. K., Cheung, T., and Yin, J. H. (2007). "Influence of degree of saturation on soil nail pull-out resistance in compacted completely decomposed granite fill." *Canadian Geotechnical Journal*, Vol. 44, No. 11, pp. 1314-1328.
- Tan, Y. and Chow, C. (2004). "Slope stabilization using soil nails: design assumptions and construction realities." *Malaysia-Japan Symposium on Geohazards and Geoenvironmental Engineering*, Bangi, Malaysia.
- Turner, J. P. and Jensen, W. G. (2005). "Landslide stabilization using soil nail and mechanically stabilized earth walls: Case study." *Journal of Geotechnical and Geoenvironmental Engineering*, Vol. 131, No. 2, pp. 141-150.
- Wang, Z. and Richwien, W. (2002). "A study of soil-reinforcement interface friction." *Journal of Geotechnical and Geoenvironmental Engineering*, Vol. 128, No. 1, pp. 92-94.
- Xue, X., Yang, X., and Liu, E. (2013). "Application of modified Goodman model in soil nailing." *International Journal of Geomechanics*, Vol. 13, No. 1, pp. 41-48.
- Yin, J. H. and Su, L. J. (2006). "An innovative laboratory box for testing nail pull-out resistance in soil." *ASTM Geotechnical Testing Journal*, Vol. 29, No. 6, pp. 1-11.